ELSEVIER

Contents lists available at ScienceDirect

Materials Today Energy

journal homepage: www.journals.elsevier.com/materials-today-energy/



Off-stoichiometric design of a manganese-rich mixed olivine Li-ion cathode for improved specific energy



Angel Burgos ^a, Junteng Du ^a, Danna Yan ^a, Yazhou Zhou ^a, Hannah Levy ^b, Jeong Gi Ryu ^c, Iae Chul Kim ^{a,*}

- ^a Department of Chemical Engineering and Materials Science, Stevens Institute of Technology, Hoboken, NJ, USA
- ^b Department of Chemical Engineering, University of Florida, Gainesville, FL, USA
- ^c Department of Computer Science, Stevens Institute of Technology, Hoboken, NJ, USA

ARTICLE INFO

Article history:
Received 24 May 2024
Received in revised form
17 July 2024
Accepted 31 July 2024
Available online 9 August 2024

Keywords: Lithium iron phosphate Mn-rich Off-stoichiometric compounds Particle dispersion

ABSTRACT

Lithium phospho-olivine cathodes operating with iron (Fe) and manganese (Mn) redox centers are considered technologically important materials that can make the development of Li-ion batteries sustainable. Although large Mn content is desirable to achieve high specific energy at a material level, the mixed olivine cathodes require particle nanostructuring and post-synthesis treatment to demonstrate reasonable energy storage properties at an electrode level. In this work, we have investigated the effect of off-stoichiometry on the electrochemical properties of a Mn-rich mixed olivine cathode material that does not require complex optimization processing. An off-stoichiometric form of LiFe_{0.25}Mn_{0.75}PO₄ is synthesized with nominal composition of LiFe_{0.225}Mn_{0.675}PO_{9.95}O_{3.8}. X-ray diffraction and electron microscopy indicate that off-stoichiometry leads to phase separation into stoichiometric LiFe_{0.25}Mn_{0.75}PO₄ crystalline particles with non-crystalline surface phases. The off-stoichiometric cathode has an improved specific energy of 622 Wh/kg at C/5, outperforming the stoichiometric cathode. The off-stoichiometric cathode also exhibits improved rate capability, delivering 120 mAh/g at 20C and 78 mAh/g at 40C discharge, respectively, due to reduced interfacial and charge transfer resistances. This work highlights off-stoichiometry as an effective approach to engineer Mn-rich mixed olivine cathode materials with mixed electrochemical properties, providing a practically feasible route for materials optimization.

© 2024 Elsevier Ltd. All rights are reserved, including those for text and data mining, Al training, and similar technologies.

1. Introduction

Designing cathode materials comprised of non-critical, earth-abundant elements is key in the sustainable growth of high-demand lithium (Li)-ion battery applications. In particular, olivine-type lithium iron phosphate (LiFePO₄) has shown great promise toward developing a stable and affordable battery material [1,2]. If optimized, the LiFePO₄ cathode that operates at 3.4 V can deliver near theoretical capacity (170 mAh/g) [3,4]. To achieve specific energy beyond what LiFePO₄ can offer, mixed olivine compositions of LiFe_{1-x}Mn_xPO₄ (0 < x < 1) have been explored to leverage high average redox potential of Mn^{2+/3+} (~4.1 V) at the same capacity [5–7].

* Corresponding author. E-mail address: jkim7@stevens.edu (J.C. Kim). The specific energy of the mixed olivine cathodes obtained, however, does not scale with the Mn composition in practice. As LiMnPO₄ is known to have poor electrical conductivity and unstable charged state [8], Mn-rich mixed olivine cathodes tend to inherit poor rate capability and short cycle life [9]. For instance, pristine LiFe_{0.25}Mn_{0.75}PO₄, in which theoretical specific energy is 670 Wh/kg, fails to deliver more than 600 Wh/kg above slow charge and discharge rates (e.g., C/20) [1,10,11]. Mixed olivine cathode compositions with higher Mn content (x > 0.75) result in even further reduced capacity and specific energy [1,10]. While the fundamental origin of this rate-limited electrochemical properties for mixed olivine cathodes is yet to be fully confirmed, it has been demonstrated that tailoring particle morphology via complex nanostructuring, doping, and/or coating can enhance their Li intercalation properties [7,12,13].

Off-stoichiometric composition design that does not introduce complexity in synthesis can result in desirable electrochemical properties. An excess amount of lithium and phosphorous relative to transition metals may induce phase separation into stoichiometric olivine and Li-rich phosphate phases, as dictated by their phase diagrams [14,15]. Upon synthesis, LiFePO₄ and LiMnPO₄ particles can be nanosized and encapsulated by poorly crystallized Li- and phosphate-rich surface phases that are ion-conductive, enabling superior rate capability to their pristine states [14–16]. The off-stoichiometric composition has also been applied to an Ferich mixed olivine LiFe_{0.6}Mn_{0.4}PO₄ cathode, delivering 135 mAh/g at 5C discharge, 57% more than what the stoichiometric cathode can offer (86 mAh/g) [17]. The average discharge voltage was also seen to increase due to improved Li kinetics. At C/5, the off-stoichiometric LiFe_{0.6}Mn_{0.4}PO₄ cathode delivered 605 Wh/kg, whereas the stoichiometric one exhibited 558 Wh/kg [17].

Although proven effective, off-stoichiometric composition design has been underutilized in developing mixed olivine cathodes. To push the limit of the Mn content, we herein propose off-stoichiometric LiFe_{0.25}Mn_{0.75}PO₄ for improved specific energy and reversibility without any post-synthesis treatment. Off-stoichiometry for Li: transition metals: phosphate is set as 1: 0.9: 0.95, while the Fe: Mn ratio is kept at 1: 3. Our off-stoichiometric LiFe_{0.25}Mn_{0.75}PO₄ cathode exhibits improved rate capability, 160 mAh/g at C/5, 150 mAh/g at 1C, and 120 mAh/g at 20C, with excellent capacity retention, outperforming the stoichiometric cathode. We consider that off-stoichiometric compositions can effectively promote fast Li transport kinetics of Mn-rich mixed olivine cathodes at an electrode level, enabling the sustainable development of Li-ion batteries.

2. Experimental

2.1. Materials preparation

We synthesized Mn-rich mixed olivine compounds by a solid-state route. Li $_2$ CO $_3$ (\geq 99.0%, Sigma-Aldrich), FeC $_2$ O $_4\cdot 2H_2$ O (99.999%, Alfa Aesar), MnC $_2$ O $_4\cdot 2H_2$ O (\geq 97.7%, Thermo Scientific), and NH $_4$ H $_2$ PO $_4$ (99.995%, Thermo Scientific) were measured to obtain stoichiometric and off-stoichiometric olivines with nominal compositions of LiFe $_{0.25}$ Mn $_{0.75}$ PO $_4$ and LiFe $_{0.225}$ Mn $_{0.675}$ PO $_{0.95}$ O $_3$ 8, respectively. The precursors were dispersed into acetone and ball-milled with zirconia balls at 300 rpm for 24 h. After drying, the mixtures were fired in two steps at 350 °C for 10 h in argon and at 650 °C for 10 h in argon with intermediate grinding.

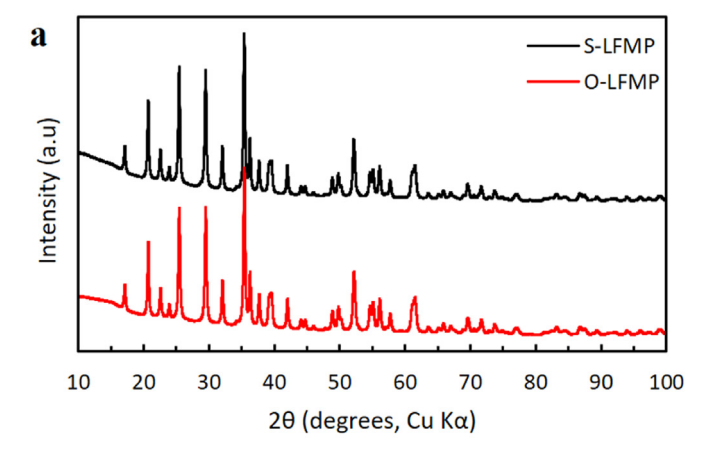
2.2. Characterization

The crystal structure of the synthesized materials was characterized by X-ray diffraction (XRD, Rigaku Miniflex IV, Cu Kα). Particle size and morphology were analyzed by scanning electron microscopy (SEM, Zeiss Auriga) and transmission electron microscopy (TEM, JEOL 2100 Plus). To evaluate electrochemical properties, we used Swagelok-type cells and 2032-coin cells. Dry-mixed cathodes consisting of the mixed-olivine (80 wt%), carbon black (15 wt%), and polytetrafluoroethylene (5 wt%) were combined with the Li metal anode, a Celgard separator, and a carbonate electrolyte (1 M LiPF₆ in ethylene carbonate and dimethyl carbonate, Sigma-Aldrich). Cathode loading density was approximately 2 mg/cm². The cells were galvanostatically cycled at various current densities in 2.5–4.5 V, where the 1C rate is based on one-electron theoretical capacities for stoichiometric and off-stoichiometric cathodes, 170 and 165 mA/g, respectively. Rate capability was evaluated at C/5, 1C, 20C, and 40C discharge consecutively after intermediate C/5 charge. Electrochemical impedance spectroscopy (EIS) was performed in the frequency 7 MHz-100 mHz. All electrochemical properties were measured at 25 °C.

3. Results and discussion

Fig. 1a shows the XRD pattern of an as-synthesized off-stoichiometric mixed olivine composition, LiFe_{0.225}Mn_{0.675}P_{0.95}O_{3.8} (O-LFMP), and its comparison to that of a stoichiometric olivine composition, LiFe_{0.25}Mn_{0.75}PO₄ (S-LFMP). Peak positions, shapes, and relative intensity ratios for O-LFMP are identical to those of S-LFMP, indicating that the stoichiometric olivine phase is formed regardless of off-stoichiometry. Using the reference olivine crystal structure (the space group Pnma), Rietveld refinement of the XRD pattern obtained from O-LFMP in Fig. 1b suggests that its lattice parameters are a=10.4058 Å, b=6.0721 Å, and c=4.7286 Å. This result is consistent with Rietveld-refined lattice parameters of S-LFMP, a=10.4126 Å, b=6.0770 Å, c=4.7320 Å (Fig. S1), as well as in good agreement with previous findings in literature [17,18]. The Rietveld refinement results are summarized in Tables S1 and S2.

Fig. 2a and b show SEM images of as-synthesized O-LFMP and S-LFMP, respectively. Both materials have similar particle size distribution with an average primary particle size of approximately 50 nm. Those primary particles for both materials tend to form agglomerated secondary particles, in which size ranges from 200 to 600 nm. Particle shape distributions are random without optimization. High resolution TEM (HRTEM) can clearly reveal differences in surface configuration between the two particles. The O-LFMP particle shown in Fig. 2c has a 6 nm-thick, non-crystalline surface layer conformally covering the crystalline phase. In contrast, the surface layer is unobservable for the S-LFMP particle in Fig. 2d.



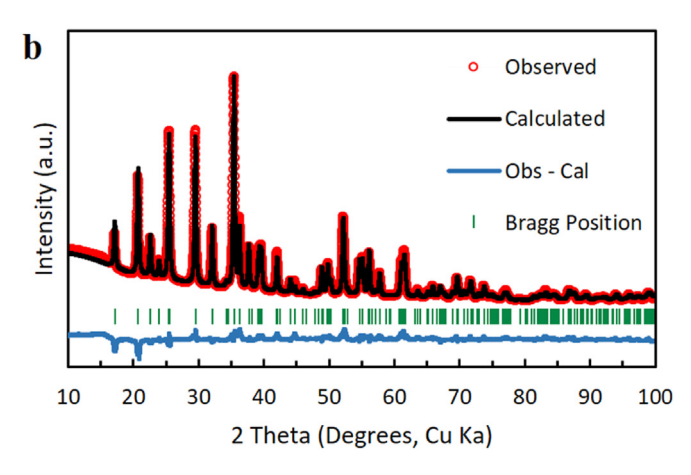


Fig. 1. (a) XRD patterns of LiFe $_{0.225}$ Mn $_{0.675}$ P $_{0.95}$ O $_{3.8}$ (O-LFMP) and LiFe $_{0.25}$ Mn $_{0.75}$ PO $_4$ (S-LFMP) and (b) the Rietveld refined XRD profile for O-LFMP.

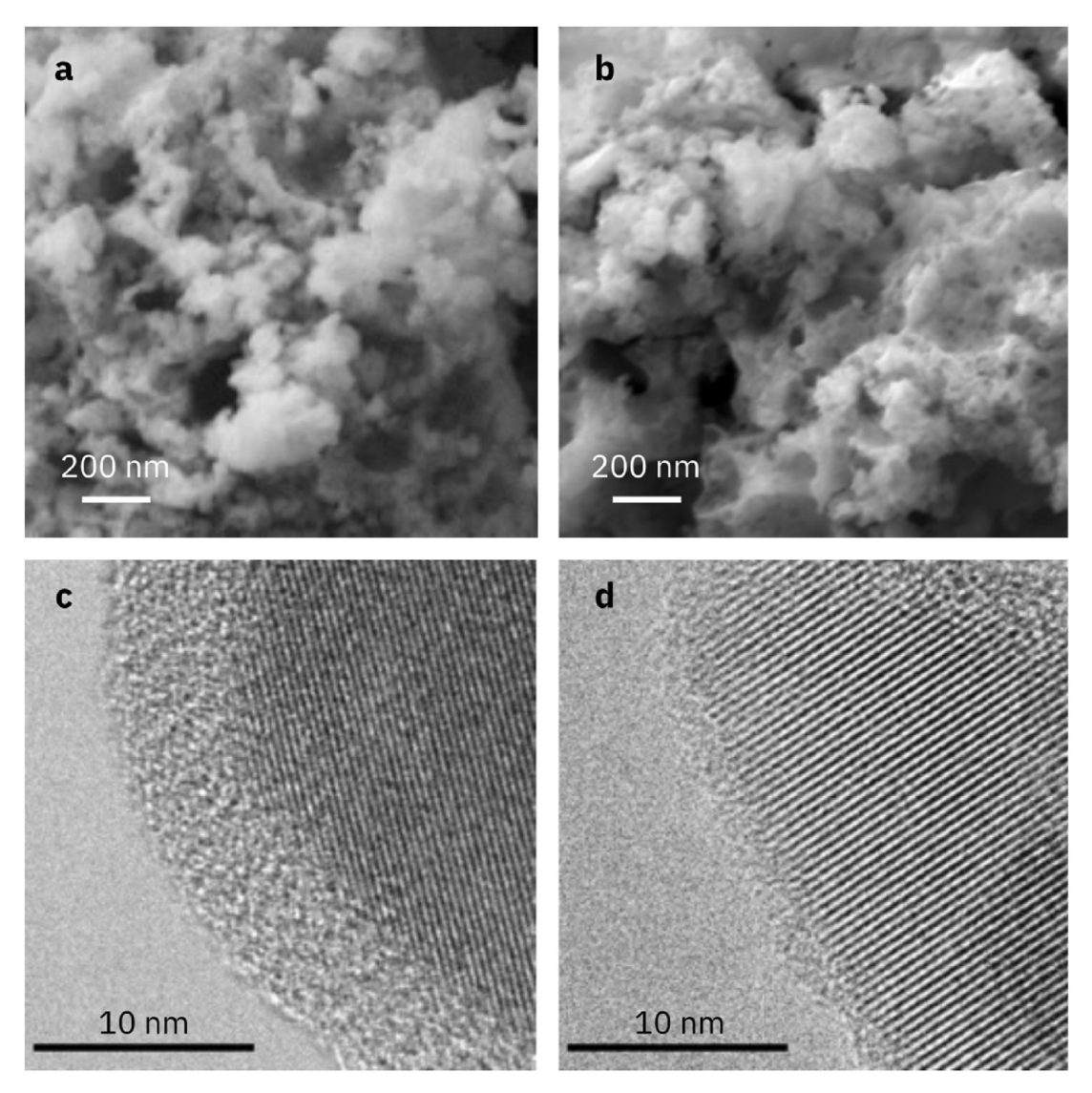


Fig. 2. SEM images of as-synthesized (a) O-LFMP and (b) S-LFMP particles. HRTEM images of (c) O-LFMP and (d) S-LFMP.

Taken together, we conclude that off-stoichiometry in $\text{LiFe}_{0.225}\text{Mn}_{0.675}\text{P}_{0.95}\text{O}_{3.8}$ leads to the formation of crystalline, stoichiometric $\text{LiFe}_{0.25}\text{Mn}_{0.75}\text{PO}_4$ olivine particles, while the excess elements remain non-crystalline in surface. Similar results were also observed for off-stoichiometric LiFePO_4, LiMnPO_4, and their Fe-rich solid solution [14,16,17]. While the origin of this peculiar particle morphology remains undiscovered, kinetics of phase transformations may govern how the particle forms, though no solid evidence exists due to limited availability to monitor solid-state synthesis. We suspect that the olivine phase may crystallize sequentially by nucleation of transition metal phosphate and subsequent lithiation, making remaining lithium phosphate and/or pyrophosphate, as dictated by the off-stoichiometric ratio, decorate the surface of the olivine phase.

Fig. 3a shows voltage vs. capacity profiles of the O-LFMP cathode at the 1st, 10th, 52nd, and 110th cycles. The cell was galvanostatically charged and discharged at C/5. Two voltage plateaus are observed at 3.55 V and 4.2 V upon charge, and at 3.5 V and 4 V upon discharge, indicative of reversible $Fe^{2+/3+}$ and $Fe^{2+/3+}$ redox reactions. In Fig. S2, polarization in Mn redox observed for O-LFMP is smaller than that for S-LFMP, while polarization in Fe redox is

nearly the same for both materials. This suggests that kinetic improvement is largely within the Mn part. Capacity retention as a function of cycle number at room temperature is also plotted in Fig. 3b. The capacity value obtained is 150 mAh/g at the 1st discharge but increases gradually to 158 mAh/g at the 10th cycle. With fluctuation, discharge capacity reaches 164 mAh/g, closely matching its theoretical capacity (165 mAh/g) at the 52nd cycle. The capacity fluctuation in early cycles may be related to the development of solid-electrolyte interphases (SEIs), gradual separator wetting, and/or progressive electrolyte permeation into the cathode particles [19–22]. Discharge capacity obtained at the 110th cycle is 160 mAh/g, demonstrating excellent reversibility, unlike other Mn-rich olivine cathodes that show limited cycle life in literature [9].

Fig. 3c compares capacity variation of O-LFMP and S-LFMP cycled at different rates. O-LFMP and S-LFMP exhibit comparable discharge capacities, 160 mAh/g and 158 mAh/g, respectively, at C/5. In mixed olivine systems with high Mn content, Mn redox is the rate-limiting step due to sluggish charge transport kinetics and/or instability of the trivalent Mn state. Hence, as the rate increases, O-LFMP that exhibits improved Li intercalation kinetics at Mn redox

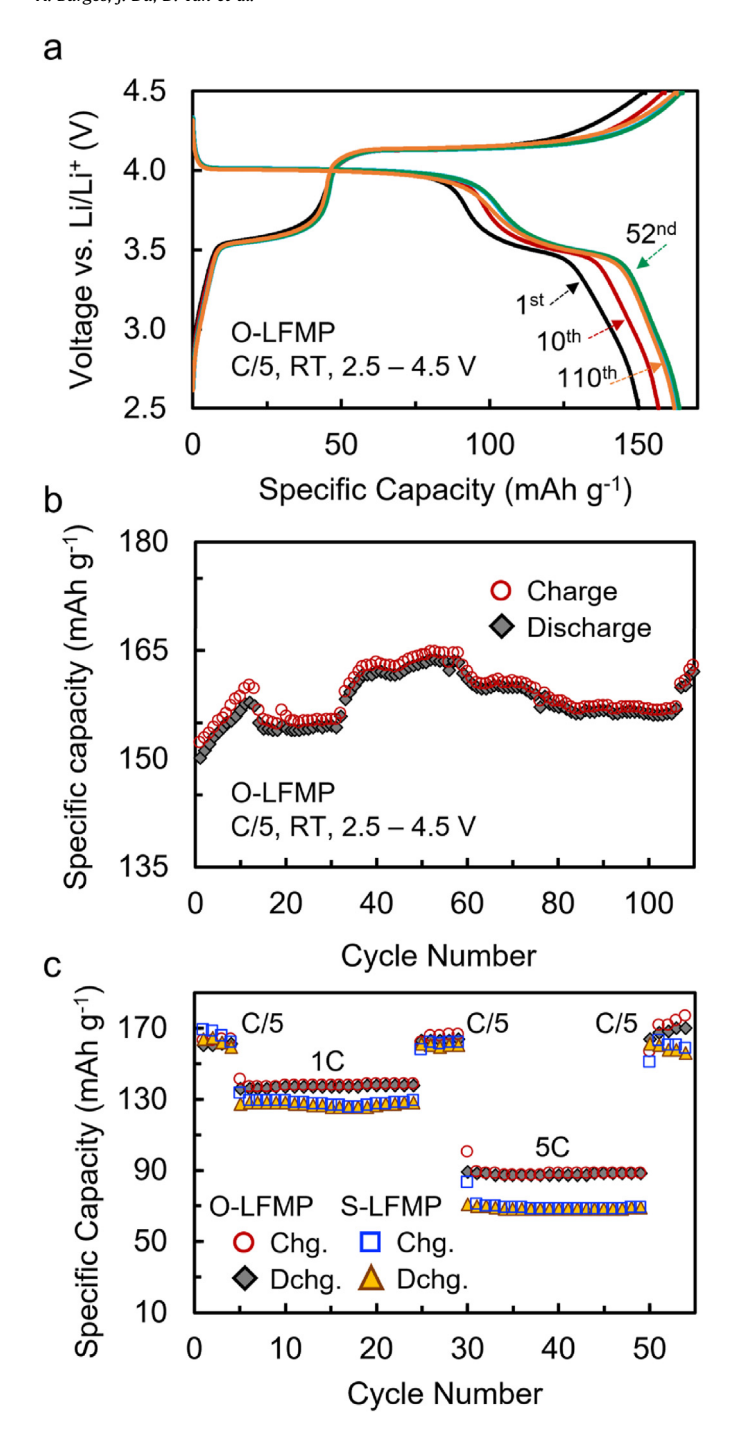


Fig. 3. (a) Voltage vs. capacity profiles of O-LFMP at 1st, 10th, 52nd, and 110th cycles, (b) specific capacity of O-LFMP as a function of cycle number, and (c) specific capacity of O-LFMP and S-LFMP cycled at varying rates.

starts to outperform S-LFMP. O-LFMP delivers 140 mAh/g at 1C discharge and 90 mAh/g at 5C discharge, whereas S-LFMP shows 130 mAh/g at 1C and 70 mAh/g at 5C. The O-LFMP cathode demonstrates higher average discharge voltage than S-LFMP due to extended Mn redox at 4 V even at C/5, as shown in Fig. 4. How voltage of the O-LFMP cathode changes as a function of capacity reflects the redox composition, in which ~28% of capacity corresponds to Fe^{2+/3+} at 3.5 V and ~72% to Mn^{2+/3+} at 4 V. This is not the case for S-LFMP where Mn redox is deferred at lower voltage due to

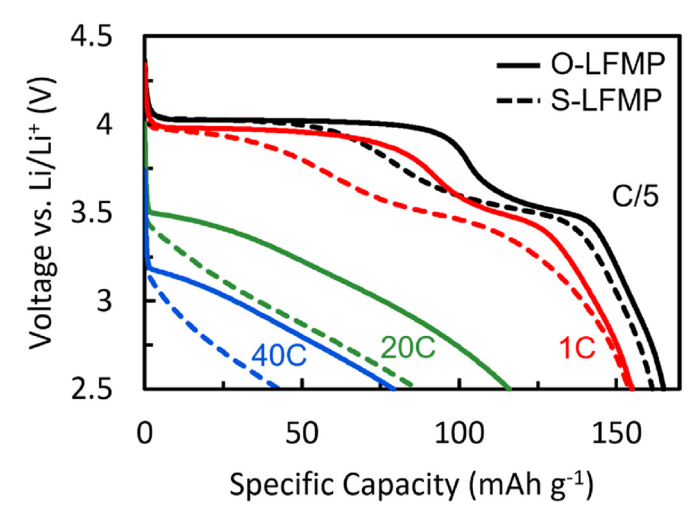


Fig. 4. Voltage vs. capacity profiles of O-LFMP and S-LFMP at various rates.

polarization, resulting in a gradual voltage transition from 4 V to 3.5 V with a shorter voltage plateau at 4 V. As a result, O-LFMP delivers 622 Wh/kg, which is 96% of its theoretical specific energy, at C/5 discharge in comparison to 598 Wh/kg for S-LFMP. The cells start to develop polarization that leads to capacity decrease at 1C. Substantially large voltage polarization at rates higher than 1C makes the 4 V plateau of O-LFMP disappear. Still, O-LFMP exhibits 120 mAh/g at 20C and 78 mAh/g at 40C. For S-LFMP, the voltage polarization is substantially greater than that of O-LFMP, leading to smaller discharge capacities, 95 mAh/g at 20C and 43 mAh/g at 40C.

We performed EIS to better understand contributions of Mn and Fe redox reactions to the cell impedance. Fig. 5a and b shows Nyquist plots of the O-LFMP cell partially discharged to 4.1 V and 3.5 V at C/5, respectively. To account for impedance from the noncrystalline surface phases in the O-LFMP particles, a parallel segment of a resistor (R_{NC}) and a constant phase element (Q_{NC}) was inserted in series to a conventional Randles circuit that models electrolyte resistance (R_S), SEI formation (R_{SEI} and Q_{SEI}), charge transfer (R_{CT}), double-layer capacitance (Q_{DL}), and bulk Li diffusion in the cathode (W) of the cell, as shown in the inset. The total resistance estimated at Mn and Fe redox are 584 Ω and 612 Ω , respectively. If fully discharged, the cell resistance is 632 Ω . For S-LFMP, the complex impedance at 4.1 V and 3.5 V are shown in Fig. 5c and d, in which cell resistance are as 556 Ω and 571 Ω , respectively. Note that the R_{NC}-Q_{NC} segment was excluded in the equivalent circuit for S-LFMP as the surface phases were unobservable. The resistance of this cell at full discharge is 579 Ω . Overall, the total cell resistance values estimated for O-LFMP are ~7% larger than those of S-LFMP at all states of discharge, due to the additional surface phases. However, the resistance contributions from each equivalent circuit element shown in Fig. 5e and listed in Tables S3 and S4 suggest that O-LFMP develops smaller R_{SEI} and R_{CT} than S-LFMP.

Improved rate capability and the resulting power density of the O-LFMP cathode can be related to its particle configuration. Upon synthesis, O-LFMP forms a de facto composite consisting of crystalline olivine particles encapsulated by non-crystalline surface phases. As dictated by the non-stoichiometric composition, and also observed in literature [14,16,17], lithium and phosphorous can be the main constituents of the surface phase. Because lithium phosphate and pyrophosphate have excellent electrochemical stability against oxidation, their passivation of the olivine particles can suppress the formation of cathode-electrolyte interphases (CEIs) at

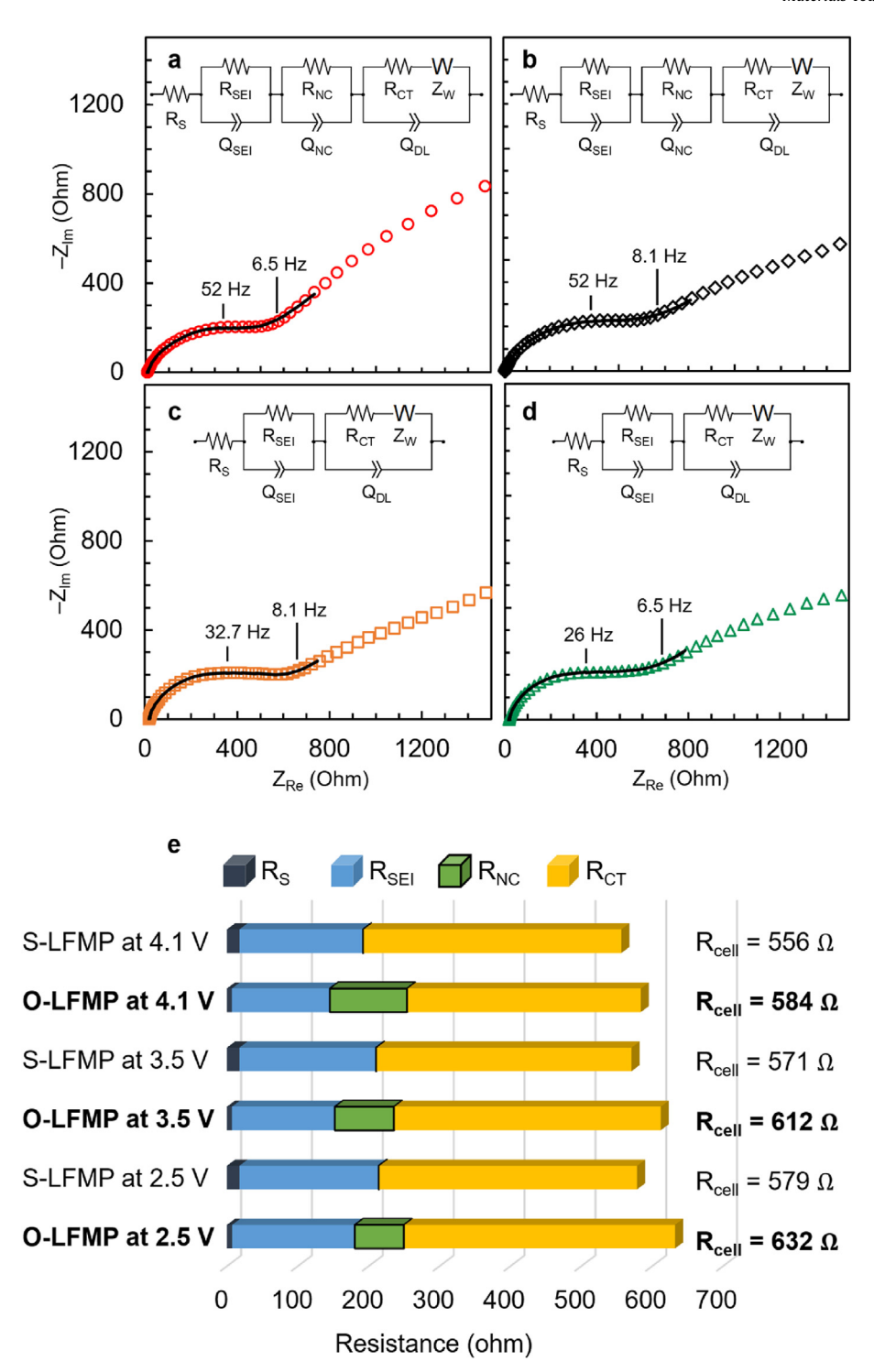


Fig. 5. Nyquist plots of the O-LFMP cathode at (a) 4.1 V and (b) 3.5 V and the S-LFMP cathode at (c) 4.1 V and (d) 3.5 V and (e) their estimated cell resistance components. Observed data is represented as points while fitted data is shown as solid lines.

high state of charge over multiple cycles [23,24]. Smaller R_{SEI} observed for O-LFMP, as combined contributions from cathodic and anodic interphases, can reflect this stability. In addition, the Li-rich non-crystalline passivation likely create percolated Li diffusion pathways across the particle-electrolyte interface within the agglomerated primary particles, promoting effective tortuosity that enables facile Li transport within the cathode. Fig. 6 shows the

specific energy of O-LFMP obtained in this work, compared with previous reports in literature [17,25–30]. The value (622 Wh/kg) obtained for O-LFMP is at C/5 discharge without particle morphology optimization and electrolyte modification, whereas others are at much slower rates (e.g., C/10 or C/20) with cathode and/or electrolyte engineering. This suggests the effectiveness of the off-stoichiometric design to develop Mn-rich olivine cathodes.

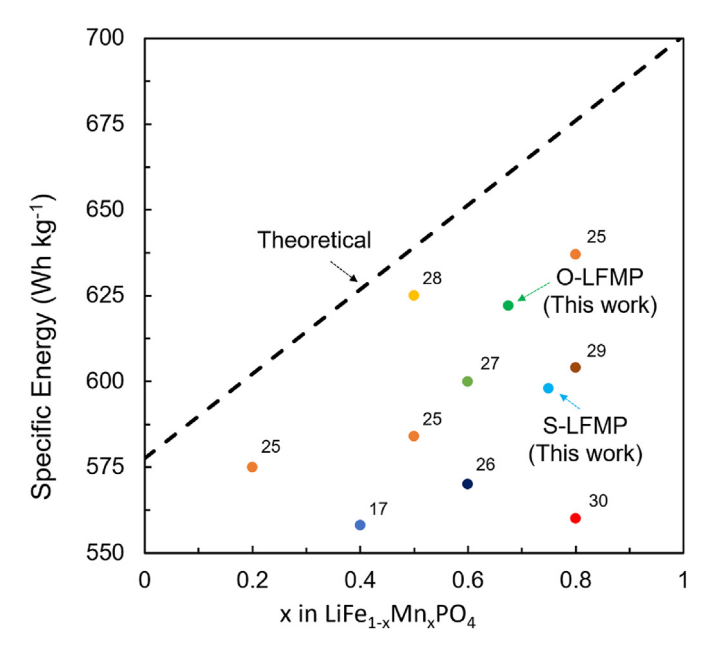


Fig. 6. Reported specific energies for different mixed olivine compositions. The dashed line represents the theoretical specific energy at a given stoichiometric composition [17,25–30].

4. Conclusions

We have applied off-stoichiometry to a mixed olivine composition with high Mn content to enhance specific energy and specific power of LiFePO₄. While it has proven challenging to leverage Mn redox for Mn-rich olivine cathodes at a practical rate, our LiFe_{0.225}Mn_{0.675}P_{0.95}O_{3.8} demonstrates full Li interaction over the extended number of cycles, delivering 622 Wh/kg at C/5 discharge. The off-stoichiometric composition forms crystalline olivine LiFe_{0.25}Mn_{0.75}PO₄ particles, in which surface is conformally covered by non-crystalline Li-rich phosphate phases during synthesis. We believe that reversible and facile Li intercalation across the offstoichiometric cathode is enabled by the surface passivation that can stabilize the cathode-electrolyte interfaces for nanosized primary particles and provide percolated Li conduction pathways within the agglomerated secondary particles. Our work highlights off-stoichiometry as an effective strategy to develop high-rate capable Mn-rich olivine cathodes.

CRediT authorship contribution statement

Angel Burgos: Writing — review & editing, Writing — original draft, Visualization, Validation, Methodology, Investigation, Formal analysis, Conceptualization. **Junteng Du:** Writing — review & editing, Formal analysis, Conceptualization. **Danna Yan:** Writing — review & editing, Visualization, Investigation. **Yazhou Zhou:** Writing — review & editing, Visualization, Investigation. **Hannah Levy:** Writing — review & editing, Investigation, Formal analysis. **Jeong Gi Ryu:** Writing — review & editing, Formal analysis. **Jae Chul Kim:** Writing — review & editing, Visualization, Supervision, Resources, Conceptualization.

Declaration of competing interest

The authors declare that they have no known competing financial interests or personal relationships that could have appeared to influence the work reported in this paper.

Data availability

Data will be made available on request.

Acknowledgment

The authors are grateful for support from the PSEG Foundation to advance energy research at Stevens Institute of Technology. H.L. was supported by the NSF REU/RET grant # 2050921.

Appendix A. Supplementary data

Supplementary data to this article can be found online at https://doi.org/10.1016/j.mtener.2024.101658.

References

- A.K. Padhi, K.S. Nanjundaswamy, J.B. Goodenough, Phospho-olivines as positive-electrode materials for rechargeable lithium batteries, J. Electrochem. Soc. 144 (4) (1997) 1188, https://doi.org/10.1149/1.1837571.
- [2] J.P. Pender, G. Jha, D.H. Youn, J.M. Ziegler, I. Andoni, E.J. Choi, A. Heller, B.S. Dunn, P.S. Weiss, R.M. Penner, C.B. Mullins, Electrode degradation in lithium-ion batteries, ACS Nano 14 (2) (2020) 1243–1295, https://doi.org/10.1021/acsnano.9b04365.
- [3] X. Lei, H. Zhang, Y. Chen, W. Wang, Y. Ye, C. Zheng, P. Deng, Z. Shi, A three-dimensional LiFePO₄/carbon nanotubes/graphene composite as a cathode material for lithium-ion batteries with superior high-rate performance, J. Alloys Compd. 626 (2015) 280–286, https://doi.org/10.1016/j.jallcom.2014.09.169.
- [4] P. Muzhikara Pratheeksha, E. Hari Mohan, B. Venkata Sarada, M. Ramakrishna, K. Hembram, P.V. Venkata Srinivas, P. Joseph Daniel, T. Narasinga Rao, S. Anandan, Development of a novel carbon-coating strategy for producing core—shell structured carbon coated LiFePO₄ for an improved Li-ion battery performance, Phys. Chem. Chem. Phys. 19 (1) (2017) 175—188, https://doi.org/10.1039/C6CP06923A.
- [5] V. Aravindan, J. Gnanaraj, Y.-S. Lee, S. Madhavi, LiMnPO₄ a next generation cathode material for lithium-ion batteries, J. Mater. Chem. A 1 (11) (2013) 3518–3539, https://doi.org/10.1039/C2TA01393B.
- [6] A. Yamada, Y. Kudo, K.-Y. Liu, Phase diagram of Li_x(Mn_yFe_{1-y})PO₄ (0 ≤ x, y ≤ 1),
 J. Electrochem. Soc. 148 (10) (2001) A1153, https://doi.org/10.1149/11401083
- [7] Y. Deng, C. Yang, K. Zou, X. Qin, Z. Zhao, G. Chen, Recent Advances of Mn-Rich LiFe_{1-y}Mn_yPO₄ (0.5 $\leq y <$ 1.0) Cathode Materials for High Energy Density Lithium Ion Batteries, Advanced Energy Materials 7 (13) (2017) 1601958. https://doi.org/10.1002/aenm.201601958.
- [8] C. Delacourt, L. Laffont, R. Bouchet, C. Wurm, J.-B. Leriche, M. Morcrette, J.-M. Tarascon, C. Masquelier, Toward understanding of electrical limitations (electronic, ionic) in LiMPO₄ (M=Fe, Mn) electrode materials, J. Electrochem. Soc. 152 (5) (2005) A913, https://doi.org/10.1149/1.1884787.
- [9] L. Yang, W. Deng, W. Xu, Y. Tian, A. Wang, B. Wang, G. Zou, H. Hou, W. Deng, X. Ji, Olivine LiMn_xFe_{1-x}PO₄ cathode materials for lithium ion batteries: restricted factors of rate performances, J. Mater. Chem. A 9 (25) (2021) 14214–14232, https://doi.org/10.1039/D1TA01526E.
- [10] G. Li, H. Azuma, M. Tohda, Optimized LiMnyFe_{1-y}PO₄ as the cathode for lithium batteries, J. Electrochem. Soc. 149 (6) (2002) A743, https://doi.org/ 10.1149/1.1473776.
- [11] X. Xie, B. Zhang, G. Hu, K. Du, J. Wu, Y. Wang, Z. Gan, J. Fan, H. Su, Y. Cao, Z. Peng, A new route for green synthesis of LiFe_{0.25}Mn_{0.75}PO₄/C@rGO material for lithium ion batteries, J. Alloys Compd. 853 (2021) 157106, https://doi.org/10.1016/j.iallcom.2020.157106.
- [12] S.K. Martha, J. Grinblat, O. Haik, E. Zinigrad, T. Drezen, J.H. Miners, I. Exnar, A. Kay, B. Markovsky, D. Aurbach, LiMn_{0.8}Fe_{0.2}PO₄: an advanced cathode material for rechargeable lithium batteries, Angew. Chem. Int. Ed. 48 (45) (2009) 8559–8563, https://doi.org/10.1002/anie.200903587.
- [13] J. Kim, D.-H. Seo, S.-W. Kim, Y.-U. Park, K. Kang, Mn based olivine electrode material with high power and energy, Chem. Commun. 46 (8) (2010) 1305–1307, https://doi.org/10.1039/B922133F.
- [14] B. Kang, G. Ceder, Battery materials for ultrafast charging and discharging, Nature 458 (7235) (2009) 190–193, https://doi.org/10.1038/nature07853.
- [15] A. Kayyar, H. Qian, J. Luo, Surface adsorption and disordering in LiFePO₄ based battery cathodes, Appl. Phys. Lett. 95 (22) (2009) 221905, https://doi.org/ 10.1063/1.3270106
- [16] B. Kang, G. Ceder, Electrochemical performance of LiMnPO₄ synthesized with off-stoichiometry, J. Electrochem. Soc. 157 (7) (2010) A808, https://doi.org/ 10.1149/1.3428454.
- [17] J.C. Kim, X. Li, B. Kang, G. Ceder, High-rate performance of a mixed olivine cathode with off-stoichiometric composition, Chem. Commun. 51 (68) (2015) 13279—13282, https://doi.org/10.1039/C5CC04434K.
- [18] E.B. Fredj, S. Rousselot, L. Danis, T. Bibienne, M. Gauthier, G. Liang, M. Dollé, Synthesis and characterization of LiFe $_{1-x}$ Mn $_x$ PO $_4$ (x=0.25,0.50,0.75) lithium

- ion battery cathode synthesized via a melting process, J. Energy Storage 27 (2020) 101116, https://doi.org/10.1016/j.est.2019.101116.
- [19] A.S. Westover, R.L. Sacci, N. Dudney, Electroanalytical measurement of interphase formation at a Li metal—solid electrolyte interface, ACS Energy Lett. 5 (12) (2020) 3860—3867, https://doi.org/10.1021/acsenergylett.0c01840.
- [20] A. Davoodabadi, C. Jin, D.L. Wood III, T.J. Singler, J. Li, On electrolyte wetting through lithium-ion battery separators, Extreme Mechanics Letters 40 (2020) 100960, https://doi.org/10.1016/j.eml.2020.100960.
- [21] A. Schilling, S. Wiemers-Meyer, V. Winkler, S. Nowak, B. Hoppe, H.H. Heimes, K. Dröder, M. Winter, Influence of separator material on infiltration rate and wetting behavior of lithium-ion batteries, Energ. Tech. 8 (2) (2020) 1900078, https://doi.org/10.1002/ente.201900078.
- [22] D.H. Jeon, Wettability in electrodes and its impact on the performance of lithium-ion batteries, Energy Storage Mater. 18 (2019) 139–147, https:// doi.org/10.1016/j.ensm.2019.01.002.
- [23] W.D. Richards, L.J. Miara, Y. Wang, J.C. Kim, G. Ceder, Interface stability in solid-state batteries, Chem. Mater. 28 (1) (2016) 266–273, https://doi.org/ 10.1021/acs.chemmater.5b04082.
- [24] Y. Zhu, X. He, Y. Mo, Origin of outstanding stability in the lithium solid electrolyte materials: insights from thermodynamic analyses based on firstprinciples calculations, ACS Appl. Mater. Interfaces 7 (42) (2015) 23685–23693, https://doi.org/10.1021/acsami.5b07517.

- [25] H. Xu, J. Zong, F. Ding, Z. Lu, W. Li, X. Liu, Effects of Fe²⁺ ion doping on LiMnPO₄ nanomaterial for lithium ion batteries, RSC Adv. 6 (32) (2016) 27164–27169, https://doi.org/10.1039/C6RA02977A.
- [26] J.-K. Kim, R. Vijaya, L. Zhu, Y. Kim, Improving electrochemical properties of porous iron substituted lithium manganese phosphate in additive addition electrolyte, J. Power Sources 275 (2015) 106–110, https://doi.org/10.1016/ i.jpowsour.2014.11.028.
- [27] S. Huang, W. Lin, L. Li, P. Liu, T. Huang, Z. Huang, J. Kong, W. Xiong, W. Yu, S. Ye, J. Hu, Q. Zhang, J. Liu, Pathway for high-energy density LiMnFePO₄ cathodes, Prog. Nat. Sci.: Mater. Int. 33 (1) (2023) 126–131, https://doi.org/10.1016/j.pnsc.2023.01.003.
- [28] J. Yang, C. Li, T. Guang, H. Zhang, Z. Li, B. Fan, Y. Ma, K. Zhu, X. Wang, Zero lithium miscibility gap enables high-rate equimolar Li(Mn,Fe)PO₄ solid solution, Nano Lett. 21 (12) (2021) 5091–5097, https://doi.org/10.1021/acs.nanolett.1c00957.
- [29] Z. Peng, B. Zhang, G. Hu, K. Du, X. Xie, K. Wu, J. Wu, Y. Gong, Y. Shu, Y. Cao, Green and efficient synthesis of micro-nano LiMn_{0.8}Fe_{0.2}PO₄/C composite with high-rate performance for Li-ion battery, Electrochim. Acta 387 (2021) 138456, https://doi.org/10.1016/j.electacta.2021.138456.
- [30] J. Li, C. Guo, Y. Qin, X. Ning, Ascorbic acid-assisted solvothermal synthesis of LiMn_{1-x}Fe_xPO₄/C nanoparticles for high-performance Li-ion cathode materials, Mater. Technol. 35 (9–10) (2020) 565–571, https://doi.org/10.1080/ 10667857.2020.1712533.